

Separating Shortcut Transition from Cross-Family OOD Failure in a Minimal Model

Hongmin Li^{1,2}

¹School of Life Science and Technology, Institute of Science Tokyo, Tokyo, Japan

²Department of Computational Biology and Medical Sciences, Graduate School of Frontier Sciences

li.hongmin.xa@alumni.tsukuba.ac.jp ORCID: 0000-0003-0228-0600

May 2026

Abstract

Shortcut features are often invoked to explain out-of-distribution (OOD) failure, but training correlation, learned shortcut use, and test-time failure need not coincide. We study a minimal binary model with one invariant coordinate and one family-dependent shortcut coordinate. In the deterministic regime, positive average shortcut correlation pulls logistic ERM toward positive shortcut weight, but ridge regularization keeps the classifier invariant-dominated and prevents deterministic OOD failure. When the invariant coordinate is noisy, ridge-logistic ERM switches to the shortcut rule once the training shortcut signal exceeds the invariant signal. Whether that transition causes failure depends on the held-out family: weaker shortcut correlation yields positive excess risk, and sign-flipped families yield above-chance error. Synthetic checks match these analytic regimes and show that the same training-side transition can have different held-out consequences. The model separates shortcut attraction, shortcut-rule transition, and cross-family OOD failure.

1 Introduction

Training families can contain predictive but unstable shortcuts: features that help on seen families but can induce failure once label correlations weaken or flip. This tension underlies shortcut learning and invariance-based OOD work (Geirhos et al., 2020; Peters et al., 2016; Rojas-Carulla et al., 2018; Schölkopf et al., 2021).

The surrounding literature spans several related questions. Domain adaptation and representation-alignment methods emphasize source-target mismatch (Ben-David et al., 2010; Ganin et al., 2016; Sun and Saenko, 2016), causal and invariant-prediction approaches ask which mechanisms remain stable across environments (Peters et al., 2016; Rojas-Carulla et al., 2018; Arjovsky et al., 2019; Schölkopf et al., 2021), and recent empirical or theoretical critiques show that robustness- or invariance-motivated objectives can still absorb shortcuts or fail under group shift (Gulrajani and Lopez-Paz, 2021; Krueger et al., 2021; Kamath et al., 2021; Rosenfeld et al., 2021; Sagawa et al., 2020; Koh et al., 2021; Nam et al., 2020). We focus on a narrower question: which train-side observations already indicate cross-family failure, and which do not. Existing work shows shortcut absorption, robustness gaps, or failures of invariance-motivated training. Here we isolate a different distinction inside one closed-form parameterization: shortcut attraction, a training-side transition to the shortcut rule, and the additional test-side condition that turns that transition into actual OOD failure. The aim is not to replace those broader lines of work, but to make this separation explicit in a minimal two-coordinate model. That distinction is useful because a train-side diagnostic may detect shortcut attraction or even a shortcut-rule transition without identifying whether the deployment family lies on the failure side of the test-family boundary.

We study a closed-form binary model with two observed coordinates,

$$X = (Z, S),$$

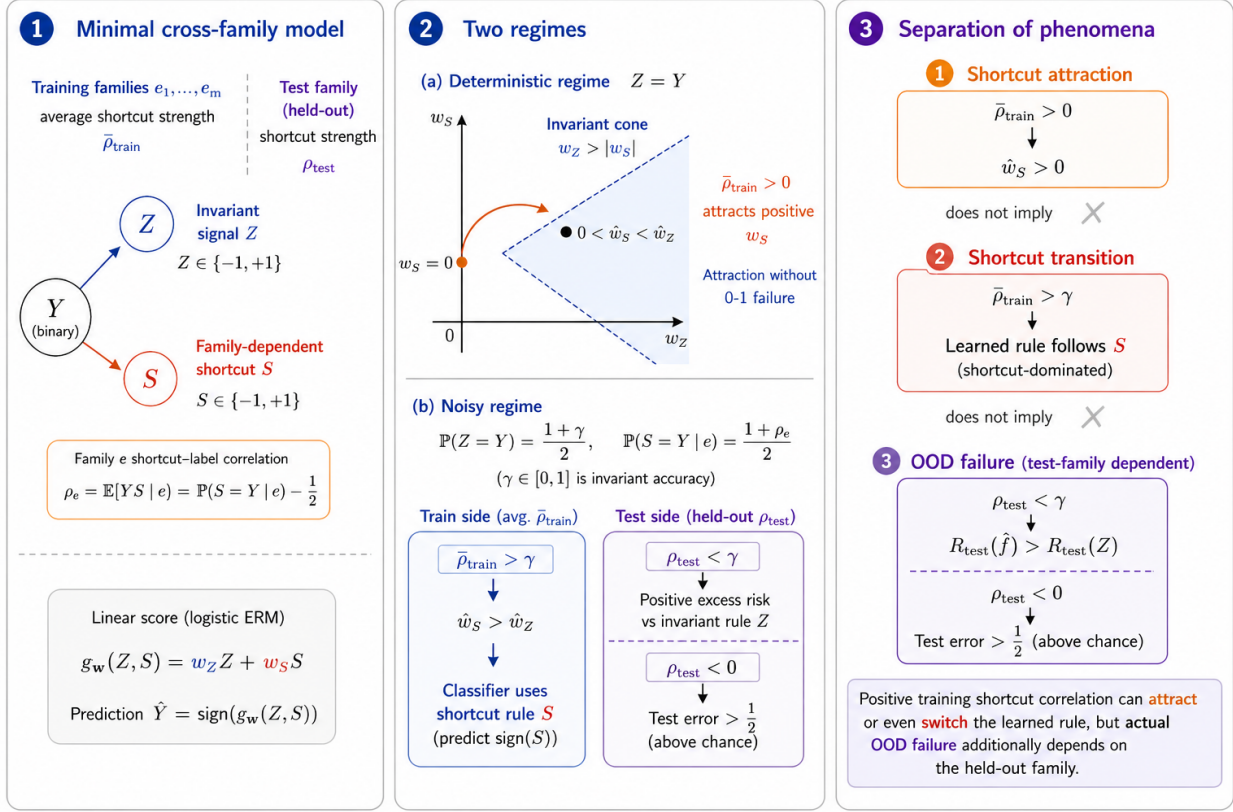


Figure 1: Main conceptual separation. The model has an invariant coordinate Z and a family-dependent shortcut coordinate S , with training families summarized by average shortcut correlation $\bar{\rho}_{\text{train}}$ and a held-out test family by ρ_{test} . Positive $\bar{\rho}_{\text{train}}$ can attract surrogate training toward a positive shortcut weight even when the deterministic classifier remains invariant-dominated. In the noisy regime, the stronger condition $\bar{\rho}_{\text{train}} > \gamma$ creates a shortcut transition, while actual cross-family OOD failure additionally depends on the held-out shortcut correlation through $\rho_{\text{test}} < \gamma$, with $\rho_{\text{test}} < 0$ giving above-chance error.

where Z is an invariant signal and S is a family-dependent shortcut. In the deterministic baseline, the true mechanism is $Y = Z$ and family e is indexed by shortcut correlation $\rho_e = \mathbb{E}_e[SY]$. Closed-form 0-1 risks and an explicit train-test gap in the shortcut cone show what positive training shortcut correlation does and does not imply: logistic ERM is pulled toward positive shortcut weight, and the test margin worsens when family correlations weaken or flip, but the ridge solution remains invariant-dominated and avoids misclassification.

To obtain a direct failure statement, we add invariant noise through independent agreement variables A and B_e with means γ and ρ_e , and set $Z = YA$, $S = YB_e$. In this regime, $\bar{\rho}_{\text{train}}$ becomes the training-side shortcut-transition parameter. The shortcut rule already beats the invariant rule when $\bar{\rho}_{\text{train}} > \gamma$, and ridge-logistic ERM obeys the same threshold. On test families with $\rho_{\text{test}} < \gamma$, that transition creates positive excess risk relative to the invariant rule; on sign-flipped families with $\rho_{\text{test}} < 0$, it yields error above chance. The same training solution can therefore be benign on one held-out family and fail on another.

Theorems 1 and 2 formalize those two steps. The deterministic theorem gives exact geometry, local shortcut incentive, and test-side degradation without claiming failure. The noisy theorem gives

the shortcut-rule transition and the additional held-out-family condition for relative or absolute failure. Figure 1 summarizes this logic, and the appendix supplies full proofs and selector-level complements.

It does not try to explain shortcut learning in general, and it does not propose a new robust training objective. Instead, it uses a minimal closed-form model to show that positive training shortcut correlation, shortcut-rule selection, and cross-family OOD failure are distinct statements. The result is a minimal analytic separation between shortcut attraction, shortcut-rule transition, and failure.

2 Model and Main Results

We work with binary labels $Y \in \{-1, +1\}$ and binary inputs $X = (Z, S) \in \{-1, +1\}^2$. The coordinate Z is the invariant signal and S is a family-specific shortcut.

Deterministic family model. For each family $e \in \mathcal{E}$, let

$$Y \sim \text{Unif}\{-1, +1\}, \quad Z = Y,$$

and

$$S = \begin{cases} Y, & \text{with probability } \frac{1+\rho_e}{2}, \\ -Y, & \text{with probability } \frac{1-\rho_e}{2}, \end{cases}$$

where $\rho_e \in [-1, 1]$ is the shortcut-label correlation of family e .

We study linear scores

$$g_w(Z, S) = w_Z Z + w_S S, \quad f_w(Z, S) = \text{sign}(g_w(Z, S)).$$

If the learner observes training families e_1, \dots, e_m with weights $\alpha_1, \dots, \alpha_m$, we write

$$\bar{\rho}_{\text{train}} := \sum_{i=1}^m \alpha_i \rho_{e_i}.$$

Exact risk geometry. Write

$$a_+ := w_Z + w_S, \quad a_- := w_Z - w_S.$$

For every family e ,

$$R_e(w) = \frac{1+\rho_e}{2} \psi(a_+) + \frac{1-\rho_e}{2} \psi(a_-),$$

where $\psi(t) = \mathbf{1}\{t < 0\} + \frac{1}{2}\mathbf{1}\{t = 0\}$. Hence the risk is piecewise constant on four cones. On the shortcut-dominated cone $w_S > |w_Z|$, the family-wise error is $(1 - \rho_e)/2$, so weaker test shortcut correlation creates an explicit train-test gap.

Away from the boundaries $a_+ = 0$ and $a_- = 0$, this becomes the explicit four-cone decomposition

$$R_e(w) = \begin{cases} 0, & w_Z > |w_S|, \\ \frac{1-\rho_e}{2}, & w_S > |w_Z|, \\ \frac{1+\rho_e}{2}, & -w_S > |w_Z|, \\ 1, & w_Z < -|w_S|. \end{cases}$$

The nonnegative shortcut cone is the one relevant for the later logistic analysis.

Averaging over training families simply replaces ρ_e by $\bar{\rho}_{\text{train}}$. Thus on the shortcut-dominated cone with $w_Z, w_S \geq 0$ and $w_S > w_Z$,

$$R_{\text{train}}(w) = \frac{1 - \bar{\rho}_{\text{train}}}{2}, \quad R_{\text{test}}(w) = \frac{1 - \rho_{\text{test}}}{2},$$

so

$$R_{\text{test}}(w) - R_{\text{train}}(w) = \frac{\bar{\rho}_{\text{train}} - \rho_{\text{test}}}{2}.$$

If the observed families make the shortcut look predictive but the test family weakens or flips that correlation, the exact cross-family gap is already positive at the level of 0-1 geometry.

Surrogate shortcut attraction. The 0-1 risk is piecewise constant, so it does not reveal the optimization bias of surrogate training. For logistic loss $\ell(t) = \log(1 + e^{-t})$, the weighted training objective is

$$L_{\text{train}}(w_Z, w_S) = \frac{1 + \bar{\rho}_{\text{train}}}{2} \ell(a_+) + \frac{1 - \bar{\rho}_{\text{train}}}{2} \ell(a_-).$$

At $w_S = 0$, with $\sigma(t) = (1 + e^{-t})^{-1}$,

$$\left. \frac{\partial L_{\text{train}}}{\partial w_S} \right|_{w_S=0} = -\bar{\rho}_{\text{train}} \sigma(-w_Z).$$

Hence every $w_Z > 0$ with $\bar{\rho}_{\text{train}} > 0$ is locally pushed toward positive shortcut weight. This deterministic scope isolates *shortcut attraction* without yet implying OOD failure.

The same formulas also expose the train-test surrogate gap. For a test family with shortcut correlation ρ_{test} ,

$$L_{\text{test}}(w_Z, w_S) - L_{\text{train}}(w_Z, w_S) = \frac{\rho_{\text{test}} - \bar{\rho}_{\text{train}}}{2} (\ell(a_+) - \ell(a_-)).$$

Hence if $w_S > 0$ and $\rho_{\text{test}} < \bar{\rho}_{\text{train}}$, the positive shortcut weight that training prefers already worsens the test surrogate.

Reparameterizing by $u = w_Z + w_S$ and $v = w_Z - w_S$. In the deterministic objective, the u channel is weighted by $(1 + \bar{\rho}_{\text{train}})/2$ and the v channel by $(1 - \bar{\rho}_{\text{train}})/2$. Positive $\bar{\rho}_{\text{train}}$ therefore stretches the u channel more than the v channel, which explains why the optimizer picks positive shortcut weight while still keeping both channels positive.

Theorem 1 (Deterministic ridge optimum). *Under the deterministic family model above, fix $0 < \bar{\rho}_{\text{train}} < 1$ and $\lambda > 0$, and let $\hat{w}^\lambda = (\hat{w}_Z^\lambda, \hat{w}_S^\lambda)$ denote the ridge-logistic minimizer. Then*

$$0 < \hat{w}_S^\lambda < \hat{w}_Z^\lambda.$$

Hence the classifier stays in the invariant cone and has zero 0-1 error on every family in the deterministic model.

Why deterministic attraction is not yet failure. The deterministic model still exposes a genuine test-side degradation. For every test family,

$$\mathbb{E}_{\text{test}} [Y g_w(X)] = w_Z + \rho_{\text{test}} w_S.$$

If $\rho_{\text{test}} < 0$ and $w_S > 0$, then the shortcut component strictly lowers the test margin relative to dropping S . Theorem 1 matters because it pins down where this degradation stops: ridge-logistic ERM absorbs positive shortcut weight but remains inside the invariant cone, so the deterministic scope gives surrogate degradation without forcing misclassification. In this regime, train-side shortcut attraction and test-side harm appear without an actual switch to the shortcut rule.

Role of ridge regularization. Without regularization, the deterministic model is linearly separable because $Z = Y$. The negative derivative at $w_S = 0$ should therefore be read as a local shortcut bias. Ridge regularization is used only to convert that local bias into a finite optimizer statement.

Passing to the noisy regime. The deterministic analysis therefore resolves only the first part of the story: whether positive average shortcut correlation creates pressure toward the shortcut coordinate. It cannot produce a shortcut-rule transition because the invariant coordinate is still perfect. To study when train-side shortcut pressure becomes actual rule selection, we keep the same two-coordinate family model and relax only the invariant signal by introducing noise level γ . This preserves the meaning of $\bar{\rho}_{\text{train}}$ as the aggregate training shortcut strength while making the invariant-shortcut comparison nontrivial.

Noisy-invariant family model. Fix $\gamma \in (0, 1]$. For each family e , let

$$Y \sim \text{Unif}\{-1, +1\},$$

let $A, B_e \in \{-1, +1\}$ be independent of Y and independent of each other, with

$$\mathbb{E}[A] = \gamma, \quad \mathbb{E}[B_e] = \rho_e,$$

and define

$$Z = YA, \quad S = YB_e.$$

If the training distribution mixes observed families e_1, \dots, e_m with weights $\alpha_1, \dots, \alpha_m$, introduce a family index

$$E \sim \sum_{i=1}^m \alpha_i \delta_{e_i},$$

independent of (Y, A) , and define the training-side shortcut agreement variable

$$B := B_E.$$

Then $\mathbb{E}[B] = \bar{\rho}_{\text{train}}$. Equivalently, for each family,

$$\mathbb{P}(Z = Y) = \frac{1 + \gamma}{2}, \quad \mathbb{P}(S = Y) = \frac{1 + \rho_e}{2}.$$

Rule-level bridge in the noisy regime. Let the invariant rule be $f_Z(z, s) = z$ and the shortcut rule be $f_S(z, s) = s$. Under the noisy model,

$$R_{\text{train}}(f_Z) = \frac{1 - \gamma}{2}, \quad R_{\text{train}}(f_S) = \frac{1 - \bar{\rho}_{\text{train}}}{2},$$

and on a test family,

$$R_{\text{test}}(f_S) - R_{\text{test}}(f_Z) = \frac{\gamma - \rho_{\text{test}}}{2}.$$

Thus the training distribution already prefers the shortcut rule exactly when $\bar{\rho}_{\text{train}} > \gamma$, which is the training-side shortcut-transition threshold. A positive test risk gap against the invariant rule appears when the test family weakens further so that $\rho_{\text{test}} < \gamma$, and sign-flipped test families with $\rho_{\text{test}} < 0$ yield error above chance. The next theorem shows that full ridge-logistic ERM over linear scores also enters the shortcut-rule side under the same training inequality, so the transition is not an artifact of comparing only two hand-picked rules.

The noisy regime also admits a direct coordinate-swap identity. If $L_{\text{train}}^{\text{noisy}}$ denotes the population noisy logistic objective, then

$$L_{\text{train}}^{\text{noisy}}(w_Z, w_S) - L_{\text{train}}^{\text{noisy}}(w_S, w_Z) = \frac{\bar{\rho}_{\text{train}} - \gamma}{2}(w_Z - w_S).$$

So when $\bar{\rho}_{\text{train}} > \gamma$, every point with $w_Z > w_S$ is worse than its coordinate-swapped version, so the noisy objective pushes the optimizer toward shortcut-rule behavior. The appendix sharpens this into an exact sign statement by showing that the sign of $\hat{w}_Z^\lambda - \hat{w}_S^\lambda$ changes at $\bar{\rho}_{\text{train}} = \gamma$.

The same threshold has a finite-sample counterpart. If $\Delta_{\text{train}} := \bar{\rho}_{\text{train}} - \gamma > 0$ and empirical risk is minimized over the two-rule class $\{f_Z, f_S\}$ on n i.i.d. draws from the family-averaged training distribution, then the shortcut rule is selected with probability at least $1 - \exp(-n\Delta_{\text{train}}^2/8)$. We keep that selector-level argument in the appendix, but mention it here because the finite-sample experiment tracks the same transition rather than introducing a new story.

Theorem 2 (Noisy ridge-logistic shortcut transition). *Under the noisy-invariant family model above, fix $\lambda > 0$ and let $\hat{w}^\lambda = (\hat{w}_Z^\lambda, \hat{w}_S^\lambda)$ denote the ridge-logistic minimizer. If $\bar{\rho}_{\text{train}} > \gamma$, then*

$$\hat{w}_Z^\lambda + \hat{w}_S^\lambda > 0, \quad \hat{w}_Z^\lambda - \hat{w}_S^\lambda < 0.$$

Hence $f_{\hat{w}^\lambda}(z, s) = s$, and on any test family

$$R_{\text{test}}(f_{\hat{w}^\lambda}) - R_{\text{test}}((z, s) \mapsto z) = \frac{\gamma - \rho_{\text{test}}}{2}.$$

In particular, if $\rho_{\text{test}} < \gamma$, this test risk gap is strictly positive, and if $\rho_{\text{test}} < 0$, then

$$R_{\text{test}}(f_{\hat{w}^\lambda}) = \frac{1 - \rho_{\text{test}}}{2} > \frac{1}{2}.$$

3 Synthetic Checks

We report two synthetic checks aligned with the theory: population geometry and finite-sample noisy ERM. They numerically test the main-text claims rather than provide benchmark coverage.

Protocol. The population panels are computed from closed-form formulas or one-dimensional root solves. For finite-sample plots we use 15 sample sizes between 20 and 600, 1400 repetitions per sample size, balanced family sampling, and 95% confidence bands across repetitions. Ridge-logistic ERM is optimized over the four sufficient binary states, so the visible uncertainty comes from Monte Carlo variation rather than a large-scale optimizer. The released supplement releases the exact figure-generation script. Regenerating the two main figures with ‘-main-only’ on a single Apple M4 Max CPU workstation with 36 GB unified memory took about 4.2 seconds, peaked at roughly 130 MB memory, and used no GPU or external cluster.

Population geometry. Figure 2 shows the two analytic regimes. The left panel reproduces Theorem 1: positive average training shortcut correlation yields positive shortcut weight while the invariant coefficient stays larger. The right panel plots the sign of $\hat{w}_S - \hat{w}_Z$ over $(\gamma, \bar{\rho}_{\text{train}})$ and recovers the exact sign boundary $\bar{\rho}_{\text{train}} = \gamma$ from the noisy analysis. Shortcut weight already appears in the deterministic scope, but shortcut-rule behavior requires the strictly stronger noisy threshold.

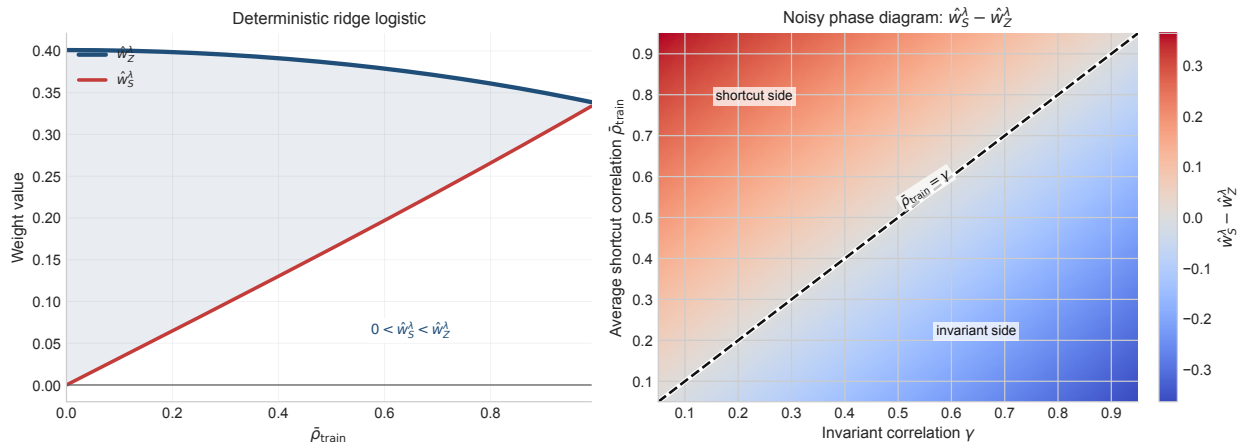


Figure 2: Population geometry. Left: deterministic ridge-logistic weights versus average training shortcut correlation. Right: noisy phase diagram via the sign of $\hat{w}_S - \hat{w}_Z$, with exact sign boundary $\bar{\rho}_{\text{train}} = \gamma$.

Finite-sample shortcut selection. Figure 3 fixes $(\gamma, \bar{\rho}_{\text{train}}) = (0.55, 0.80)$ and keeps the training distribution fixed while changing only the held-out family. The left panel tracks the training-side probability of shortcut-rule behavior. The right panel evaluates the same finite-sample estimator on two test families: a failure-side family with $\rho_{\text{test}} = -0.30$ and a no-failure control with $\rho_{\text{test}} = 0.70$. The ridge-logistic curves therefore illustrate the main separation claim directly: the training-side transition is the same in both cases, but the held-out outcome depends on the extra test-side inequality. The sign-flipped family approaches the absolute-failure side of Theorem 2, while the control family stays below both chance and the invariant baseline.

What the checks show. For this paper’s scope, Figure 2 validates the deterministic/noisy separation and the training-side sign boundary at population level, and Figure 3 shows that one shared training transition can yield different held-out outcomes depending on the test family. We therefore use the experiments as theorem-aligned sanity checks rather than as a broader empirical study of the full test-family phase diagram.

4 Discussion

The paper studies a narrow diagnostic question. Positive training shortcut correlation, learned shortcut use, and test-time failure are often discussed together, but the minimal model shows that they can come apart. Inside one closed-form parameterization, Theorem 1 shows that deterministic shortcut attraction and test-side degradation can occur without deterministic misclassification, while Theorem 2 shows what must be added before a shortcut-rule transition and cross-family failure follow. The appendix selector results reinforce the same control parameter rather than introducing a separate story.

The asymmetry between the two theorems matters. Theorem 1 is not a failure theorem; it rules out an overly strong reading of train-side evidence. Theorem 2 then adds the stronger noisy condition that actually moves ridge-logistic ERM onto the shortcut rule. Even there, the learned training solution is still not enough by itself: failure only follows after the held-out family satisfies $\rho_{\text{test}} < \gamma$, and above-chance error appears only on the stricter sign-flip side $\rho_{\text{test}} < 0$.

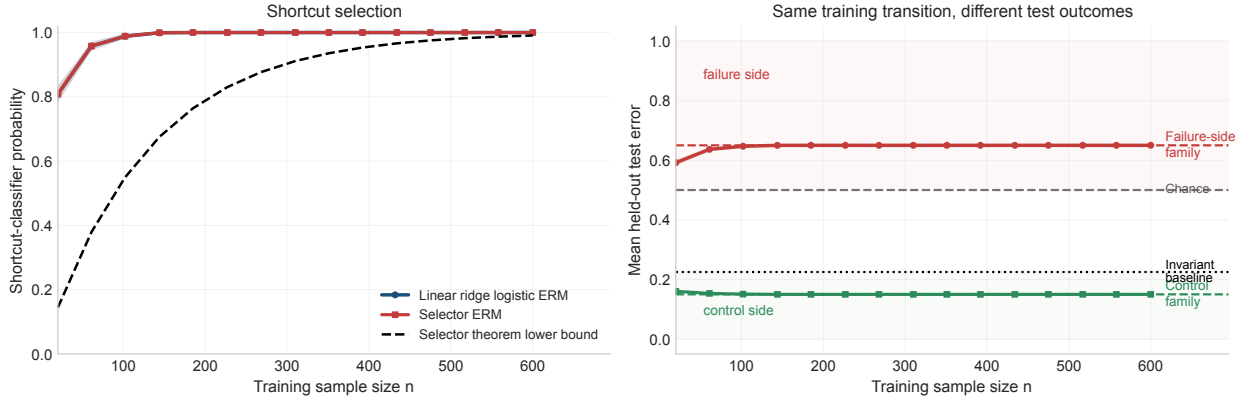


Figure 3: Finite-sample noisy ERM at fixed training setting $(\gamma, \bar{\rho}_{\text{train}}) = (0.55, 0.80)$. Left: training-side probability of shortcut-rule behavior. Right: mean test error on a failure-side family $\rho_{\text{test}} = -0.30$ and on a no-failure control $\rho_{\text{test}} = 0.70$, with invariant-rule and chance baselines.

The experiments follow the same split. Figure 2 checks the population geometry behind both regimes, while Figure 3 keeps the training distribution fixed and changes only the held-out family, so the same learned shortcut tendency can be seen producing failure-side and no-failure-side outcomes. The figures verify the separation logic of the theory; they are not benchmark evidence and do not map the full test-family phase diagram.

One modeling choice deserves emphasis. The main text parameterizes the observed training families through the average shortcut strength $\bar{\rho}_{\text{train}}$ rather than a richer family descriptor. In this minimal binary model, the exact population risk, the rule-level comparison, and the noisy training-side transition all collapse to the same family-average control parameter, while actual failure still depends on the separate test-side comparison $\rho_{\text{test}} < \gamma$. Richer family heterogeneity may matter in larger models, but that is a different problem from the one studied here.

The broader impact of this work is mainly diagnostic. Positively, clearer separation between training-side shortcut transition and test-side failure can help robustness evaluations avoid over-reading training correlations as direct deployment guarantees. Negatively, this same minimal model could be over-generalized to settings far outside its binary assumptions or used to replace empirical auditing with purely analytic arguments, which is why we keep the claims narrow and treat the figures as theorem-aligned checks rather than benchmark evidence.

5 Conclusion

This paper studies a minimal model of cross-family shortcut-driven OOD failure. Within one shared binary construction, positive training shortcut correlation can create shortcut attraction without failure, the stronger noisy inequality $\bar{\rho}_{\text{train}} > \gamma$ can move ridge-logistic ERM onto the shortcut rule, and actual test-time failure still requires a separate held-out condition $\rho_{\text{test}} < \gamma$. Sign-flipped families $\rho_{\text{test}} < 0$ then yield above-chance error.

The deterministic theorem shows why train-side shortcut evidence is not enough: attraction and surrogate degradation already appear before misclassification does. The noisy theorem adds the threshold for shortcut-rule transition, while the test family still determines whether that transition

remains benign or becomes actual OOD failure. The finite-sample check mirrors the same split under a fixed training setup.

The model is binary, the noisy regime uses independent agreement variables for invariant and shortcut coordinates, and the figures serve as theorem-aligned checks rather than benchmark evidence. Those restrictions buy exact formulas and closed-form thresholds. Extending the same separation to richer family structure is the natural next step.

References

- Martin Arjovsky, Léon Bottou, Ishaan Gulrajani, and David Lopez-Paz. Invariant risk minimization. *arXiv preprint arXiv:1907.02893*, 2019.
- Shai Ben-David, John Blitzer, Koby Crammer, and Fernando Pereira. A theory of learning from different domains. *Machine Learning*, 79(1–2):151–175, 2010.
- Yaroslav Ganin, Evgeniya Ustinova, Hana Ajakan, Pascal Germain, Hugo Larochelle, François Laviolette, Mario Marchand, and Victor Lempitsky. Domain-adversarial training of neural networks. *Journal of Machine Learning Research*, 17(59):1–35, 2016.
- Robert Geirhos, Jörn-Henrik Jacobsen, Claudio Michaelis, Richard Zemel, Wieland Brendel, Matthias Bethge, and Felix A. Wichmann. Shortcut learning in deep neural networks. *Nature Machine Intelligence*, 2(11):665–673, 2020.
- Ishaan Gulrajani and David Lopez-Paz. In search of lost domain generalization. In *International Conference on Learning Representations*, 2021.
- Pritish Kamath, Aditya Tangella, Dylan J. Sutherland, and Nathan Srebro. Does invariant risk minimization capture invariance? In *International Conference on Artificial Intelligence and Statistics*, pages 4069–4077, 2021.
- Pang Wei Koh, Shiori Sagawa, Henrik Marklund, Sang Michael Xie, Marvin Zhang, Akshay Balsubramani, Weihua Hu, Michihiro Yasunaga, Richard Phillips, Sara Beery, Jure Leskovec, and Percy Liang. WILDS: A benchmark of in-the-wild distribution shifts. In *International Conference on Machine Learning*, pages 5637–5664, 2021.
- David Krueger, Ethan Caballero, Jörn-Henrik Jacobsen, Amy Zhang, Jonathan Binas, Dinghui Zhang, Rémi Le Priol, and Aaron Courville. Out-of-distribution generalization via risk extrapolation (REx). In *International Conference on Machine Learning*, pages 5815–5826, 2021.
- Junhyun Nam, Hyuntak Cha, Sungsoo Ahn, Jaeho Lee, and Jinwoo Shin. Learning from failure: Training debiased classifier from biased classifier. In *Advances in Neural Information Processing Systems*, volume 33, pages 20673–20684, 2020.
- Jonas Peters, Peter Bühlmann, and Nicolai Meinshausen. Causal inference by using invariant prediction: Identification and confidence intervals. *Journal of the Royal Statistical Society: Series B*, 78(5):947–1012, 2016.
- Mateo Rojas-Carulla, Bernhard Schölkopf, Richard Turner, and Jonas Peters. Invariant models for causal transfer learning. *Journal of Machine Learning Research*, 19(36):1–34, 2018.
- Elan Rosenfeld, Pradeep Ravikumar, and Andrej Risteski. The risks of invariant risk minimization. *arXiv preprint arXiv:2010.05761*, 2021.

Shiori Sagawa, Pang Wei Koh, Tatsunori B. Hashimoto, and Percy Liang. Distributionally robust neural networks for group shifts: On the importance of regularization for worst-case generalization. In *International Conference on Learning Representations*, 2020.

Bernhard Schölkopf, Francesco Locatello, Stefan Bauer, Nan Rosemary Ke, Nal Kalchbrenner, Anirudh Goyal, and Yoshua Bengio. Toward causal representation learning. *Proceedings of the National Academy of Sciences*, 118(15):e2012341118, 2021.

Baochen Sun and Kate Saenko. Deep CORAL: Correlation alignment for deep domain adaptation. In *European Conference on Computer Vision Workshops*, pages 443–450, 2016.

A Appendix

B Proofs for the Main Theorems

Throughout, let

$$\ell(t) = \log(1 + e^{-t}), \quad \sigma(t) = (1 + e^{-t})^{-1}.$$

Proof of Theorem 1. Under the deterministic family model, the weighted ridge-logistic objective is

$$J_\lambda(w_Z, w_S) := \frac{1 + \bar{\rho}_{\text{train}}}{2} \ell(w_Z + w_S) + \frac{1 - \bar{\rho}_{\text{train}}}{2} \ell(w_Z - w_S) + \frac{\lambda}{2}(w_Z^2 + w_S^2).$$

Set

$$\alpha := \frac{1 + \bar{\rho}_{\text{train}}}{2}, \quad \beta := \frac{1 - \bar{\rho}_{\text{train}}}{2}, \quad u := w_Z + w_S, \quad v := w_Z - w_S.$$

Because $0 < \bar{\rho}_{\text{train}} < 1$, we have $1 > \alpha > \beta > 0$. Also

$$w_Z = \frac{u + v}{2}, \quad w_S = \frac{u - v}{2}, \quad w_Z^2 + w_S^2 = \frac{u^2 + v^2}{2}.$$

Hence

$$J_\lambda(w_Z, w_S) = \phi_\alpha(u) + \phi_\beta(v), \quad \phi_k(x) := k\ell(x) + \frac{\lambda}{4}x^2.$$

Each ϕ_k is strictly convex, with derivative

$$\phi'_k(x) = -k\sigma(-x) + \frac{\lambda}{2}x.$$

Since $\phi'_k(0) = -k/2 < 0$ and $\phi'_k(x) \rightarrow +\infty$ as $x \rightarrow +\infty$, the unique minimizer x_k^* of ϕ_k satisfies $x_k^* > 0$.

Now compare the two channels. For every x ,

$$\phi'_\alpha(x) - \phi'_\beta(x) = -(\alpha - \beta)\sigma(-x) < 0.$$

Because both derivatives are strictly increasing and each has exactly one root, their roots satisfy

$$x_\alpha^* > x_\beta^* > 0.$$

The unique minimizer of J_λ is therefore

$$u^* = x_\alpha^*, \quad v^* = x_\beta^*,$$

which implies

$$\hat{w}_S^\lambda = \frac{u^* - v^*}{2} > 0, \quad \hat{w}_Z^\lambda = \frac{u^* + v^*}{2} > \hat{w}_S^\lambda.$$

So the minimizer remains in the invariant cone. Because the deterministic model has $Z = Y$, any score with $w_Z > |w_S|$ predicts Y correctly on every family, and the resulting 0-1 error is zero. \square

Proof of Theorem 2. Under the noisy family model, define

$$A := YZ, \quad B := YS.$$

By construction, $A, B \in \{-1, +1\}$ are independent, and under the family-averaged training distribution induced by the random family index E and the mixture variable $B = B_E$,

$$\mathbb{P}(A = 1) = \frac{1 + \gamma}{2}, \quad \mathbb{P}(B = 1) = \frac{1 + \bar{\rho}_{\text{train}}}{2}.$$

Thus

$$\begin{aligned} L_{\text{train}}^{\text{noisy}}(w_Z, w_S) &:= \mathbb{E}_{\text{train}}[\ell(Y(w_Z Z + w_S S))] \\ &= \frac{(1 + \gamma)(1 + \bar{\rho}_{\text{train}})}{4} \ell(w_Z + w_S) + \frac{(1 + \gamma)(1 - \bar{\rho}_{\text{train}})}{4} \ell(w_Z - w_S) \\ &\quad + \frac{(1 - \gamma)(1 + \bar{\rho}_{\text{train}})}{4} \ell(-w_Z + w_S) + \frac{(1 - \gamma)(1 - \bar{\rho}_{\text{train}})}{4} \ell(-w_Z - w_S). \end{aligned}$$

Set again

$$u := w_Z + w_S, \quad v := w_Z - w_S.$$

Using $\ell(-t) = \ell(t) + t$, the objective separates as

$$L_{\text{train}}^{\text{noisy}}(w_Z, w_S) = \phi_u(u) + \phi_v(v),$$

where

$$\begin{aligned} \phi_u(u) &:= \frac{1 + \gamma \bar{\rho}_{\text{train}}}{2} \ell(u) + \frac{(1 - \gamma)(1 - \bar{\rho}_{\text{train}})}{4} u, \\ \phi_v(v) &:= \frac{1 - \gamma \bar{\rho}_{\text{train}}}{2} \ell(v) + \frac{(1 - \gamma)(1 + \bar{\rho}_{\text{train}})}{4} v. \end{aligned}$$

Adding the ridge penalty gives

$$J_{\lambda}^{\text{noisy}}(w_Z, w_S) = \Phi_u(u) + \Phi_v(v),$$

with

$$\Phi_u(u) := \phi_u(u) + \frac{\lambda}{4} u^2, \quad \Phi_v(v) := \phi_v(v) + \frac{\lambda}{4} v^2.$$

Each term is strictly convex, so the minimizer is unique and separates across u and v .

Differentiate:

$$\begin{aligned} \Phi'_u(u) &= -\frac{1 + \gamma \bar{\rho}_{\text{train}}}{2} \sigma(-u) + \frac{(1 - \gamma)(1 - \bar{\rho}_{\text{train}})}{4} + \frac{\lambda}{2} u, \\ \Phi'_v(v) &= -\frac{1 - \gamma \bar{\rho}_{\text{train}}}{2} \sigma(-v) + \frac{(1 - \gamma)(1 + \bar{\rho}_{\text{train}})}{4} + \frac{\lambda}{2} v. \end{aligned}$$

At the origin,

$$\Phi'_u(0) = -\frac{1 + \gamma \bar{\rho}_{\text{train}}}{4} + \frac{(1 - \gamma)(1 - \bar{\rho}_{\text{train}})}{4} = -\frac{\gamma + \bar{\rho}_{\text{train}}}{4} < 0,$$

and, because $\bar{\rho}_{\text{train}} > \gamma$,

$$\Phi'_v(0) = -\frac{1 - \gamma \bar{\rho}_{\text{train}}}{4} + \frac{(1 - \gamma)(1 + \bar{\rho}_{\text{train}})}{4} = \frac{\bar{\rho}_{\text{train}} - \gamma}{4} > 0.$$

Since Φ'_u is strictly increasing and tends to $+\infty$ as $u \rightarrow +\infty$, its unique root satisfies $u^* > 0$. Since Φ'_v is strictly increasing and tends to $-\infty$ as $v \rightarrow -\infty$, its unique root satisfies $v^* < 0$. Therefore

$$\hat{w}_Z^\lambda + \hat{w}_S^\lambda = u^* > 0, \quad \hat{w}_Z^\lambda - \hat{w}_S^\lambda = v^* < 0.$$

To identify the induced classifier, fix any $(z, s) \in \{-1, +1\}^2$. If $z = s$, then

$$\hat{w}_Z^\lambda z + \hat{w}_S^\lambda s = u^* s,$$

whose sign is s because $u^* > 0$. If $z = -s$, then

$$\hat{w}_Z^\lambda z + \hat{w}_S^\lambda s = v^* z = -v^* s,$$

whose sign is again s because $v^* < 0$. Hence

$$f_{\hat{w}^\lambda}(z, s) = s \quad \text{for every } (z, s) \in \{-1, +1\}^2.$$

On a test family, the shortcut rule therefore has risk

$$R_{\text{test}}(f_{\hat{w}^\lambda}) = \mathbb{P}_{\text{test}}(S \neq Y) = \frac{1 - \rho_{\text{test}}}{2},$$

while the invariant rule has risk

$$R_{\text{test}}((z, s) \mapsto z) = \mathbb{P}_{\text{test}}(Z \neq Y) = \frac{1 - \gamma}{2}.$$

Subtracting gives

$$R_{\text{test}}(f_{\hat{w}^\lambda}) - R_{\text{test}}((z, s) \mapsto z) = \frac{\gamma - \rho_{\text{test}}}{2}.$$

If $\rho_{\text{test}} < 0$, then also

$$R_{\text{test}}(f_{\hat{w}^\lambda}) = \frac{1 - \rho_{\text{test}}}{2} > \frac{1}{2},$$

so the learned shortcut rule fails absolutely on the shifted test family. \square

Exact sign boundary in the noisy regime. The same proof yields more than the failure-side statement in Theorem 2. Since

$$\Phi'_v(0) = \frac{\bar{\rho}_{\text{train}} - \gamma}{4},$$

strict convexity implies that the unique minimizer $v^* = \hat{w}_Z^\lambda - \hat{w}_S^\lambda$ satisfies

$$v^* \begin{cases} > 0, & \bar{\rho}_{\text{train}} < \gamma, \\ = 0, & \bar{\rho}_{\text{train}} = \gamma, \\ < 0, & \bar{\rho}_{\text{train}} > \gamma. \end{cases}$$

So the sign of $\hat{w}_Z^\lambda - \hat{w}_S^\lambda$ changes exactly at $\bar{\rho}_{\text{train}} = \gamma$, which is the boundary visualized in Figure 2.

C Supplementary Selector Results

Let

$$\mathcal{F}_{\text{sel}} = \{f_Z, f_S\}, \quad f_Z(z, s) = z, \quad f_S(z, s) = s.$$

Population selector ERM. Under the noisy-invariant family model,

$$R_{\text{train}}(f_Z) = \frac{1-\gamma}{2}, \quad R_{\text{train}}(f_S) = \frac{1-\bar{\rho}_{\text{train}}}{2}.$$

Hence if $\bar{\rho}_{\text{train}} > \gamma$, population ERM over \mathcal{F}_{sel} chooses f_S . On a test family,

$$R_{\text{test}}(f_S) - R_{\text{test}}(f_Z) = \frac{1-\rho_{\text{test}}}{2} - \frac{1-\gamma}{2} = \frac{\gamma - \rho_{\text{test}}}{2}.$$

So whenever $\rho_{\text{test}} < \gamma$, this selector-level shortcut choice incurs strictly positive OOD risk gap over the invariant rule.

Finite-sample selector ERM. Let $\Delta_{\text{train}} := \bar{\rho}_{\text{train}} - \gamma > 0$, and let

$$\hat{f}_n \in \arg \min_{f \in \mathcal{F}_{\text{sel}}} \hat{R}_n(f)$$

minimize empirical risk over n i.i.d. draws from the family-averaged training distribution. Define

$$W_i := \mathbf{1}\{f_S(X_i) \neq Y_i\} - \mathbf{1}\{f_Z(X_i) \neq Y_i\}.$$

Then $W_i \in [-1, 1]$ and

$$\hat{R}_n(f_S) - \hat{R}_n(f_Z) = \frac{1}{n} \sum_{i=1}^n W_i.$$

Moreover,

$$\mathbb{E}[W_i] = R_{\text{train}}(f_S) - R_{\text{train}}(f_Z) = \frac{\gamma - \bar{\rho}_{\text{train}}}{2} = -\frac{\Delta_{\text{train}}}{2}.$$

Applying Hoeffding's inequality,

$$\mathbb{P}(\hat{R}_n(f_S) \geq \hat{R}_n(f_Z)) \leq \exp\left(-\frac{n\Delta_{\text{train}}^2}{8}\right),$$

so

$$\mathbb{P}(\hat{R}_n(f_S) < \hat{R}_n(f_Z)) \geq 1 - \exp\left(-\frac{n\Delta_{\text{train}}^2}{8}\right).$$

On this event, $\hat{f}_n = f_S$, and therefore for any test family,

$$R_{\text{test}}(\hat{f}_n) - R_{\text{test}}(f_Z) = \frac{\gamma - \rho_{\text{test}}}{2}.$$

This is the selector-level finite-sample concentration bound referenced in the main text.